

## STORM WAVES ATTENUATION AND DAMPING PERFORMANCE OF MANGROVE FOREST - MODEL TEST RESULTS

Husrin, S.<sup>1,2</sup>, Strusińska, A.<sup>1</sup>, Hoque, A.<sup>3</sup>, Oumeraci, H.<sup>1</sup>

<sup>1</sup>Leichtweiß-Institute, Braunschweig Institute of Technology, Beethovenstr. 51a, 38106 Braunschweig, Germany,  
<sup>2</sup>Agency for Marine and Fisheries Research, Ministry of Marine and Fisheries Affairs, The Republic of Indonesia,  
Jl. Pasir putih I, Ancol 14430 Jakarta, Indonesia

<sup>3</sup> Department of Mathematics, University of Rajshahi, Rajshahi-6205 Bangladesh

### ABSTRACT

The use of coastal forest vegetations such as mangrove forests has been increasingly favoured as one of environmentally-friendly measures for coastal areas in mitigating extreme weather events such as storm waves. Though extensive laboratory studies, numerical modelling and field measurements have revealed some important aspects related to wave attenuation and flow resistance parameters, the damping performance of mangrove forests for design practice is still not fully understood. The objective of this paper is to discuss laboratory model testing results on the damping performance of mangrove forest utilizing a physically-based parameterized mangrove model. The parameterised mangrove model (scale 1:25) which consists of a group of cylinders with vertically varying submerged volume ratio ( $V_m/V$  where  $V_m$ : volume of submerged root,  $V$ : control volume) is based on quantifiable hydraulic losses to its actual prototype counterpart. Systematic laboratory experiments in the Twin Wave Flume of Leichtweiß-Institute, Technical University Braunschweig, Germany (2 m and 1 m wide, 90 m long, and 1.20 m deep) were carried out simultaneously with and without forests to investigate the attenuation of storm waves by mangrove forest as a function of forest widths, water depths, and wave conditions for both regular and irregular waves. Direct measurements using force transducers for the entire forest and for single tree models inside the forest in different configuration have revealed the evolution of hydraulic losses along the forest widths. Moreover, the damping performances of the forest model in terms of wave reflection, transmission, and energy dissipation coefficients ( $K_R$ ,  $K_T$ , and  $K_D$  respectively) have been determined for breaking and non-breaking wave conditions. Furthermore, the foreshore topography and the wave breaking locations were found to significantly influence the energy dissipation and attenuation performance of the mangrove forest.

Keywords: Storm waves, mangroves, scale-model tests, attenuation performance

### INTRODUCTION

Storm waves are generated by offshore extreme winds from tropical storms, hurricanes, typhoons, or monsoons. The rise of water level, violent waves and their long duration are the main aspects that may cause damages and widespread inundation particularly in the low lying coastal areas (Walton and Dean, 2009). Structural measures (e.g. dikes and sea walls) have been traditionally implemented to reduce the impact of storm waves. Recently, engineers and environmentalists have encouraged environmentally-friendly, nonintrusive protection measures in coastal areas such as vegetated dunes,

reefs, and coastal forests. The use of coastal forest vegetations such as mangroves has been increasingly favourable due to their widespread presence in coastal areas. Several studies claimed that mangrove forests may reduce the impact of storm waves (Massel et al. 1999). Methodologies used to support the claim are based on either field observations, laboratory experiments or analytical approaches.

Extensive field investigations on the role of mangroves (*Kandelia candel*) in reducing the impact of frequent storm waves were investigated in the coastlines of Vietnam (Mazda et al., 1997a). The relative reduction of the incident waves

travelling through a certain distance of forest width (ratio of incident and transmitted waves) was adopted as a main indicator for the attenuation performance of mangroves.

They analysed the effect of both age and density of the forest and found that the relative wave reduction is up to 20% for 6-year old mangroves and less for younger ones. The reduction rate was 10% - 15% and 1% - 3% for 3-year-old mangroves and 0.5-year-old mangroves, respectively. This study showed that water level changes did not reduce the relative wave reduction, which is not surprising due to the fact that the tree canopy in their study is generally short. Another investigation with different mangrove species (*Sonneratia sp.*) showed that the relative wave reduction was found up to 45% (tree density,  $N_s = 0.08 \text{ m}^{-2}$ ) as compared to the shore without the presence of mangroves (Mazda et al. 2006).

Wave attenuation by coastal forests has also been studied using laboratory experiments. The work of Petryk and Bosmajian (1975) on vegetation resistance in terms of Manning roughness coefficient ( $n$ ) induced by drag has been adopted for mangroves (Wolanski et al. 1980) by using a vegetation density (roots and trunks) represented by the ratio of the vegetation projected area and the area of flow through vegetation. For the case of tsunami, several laboratory studies with different parameterised mangrove tree models and different experimental set-ups were performed, resulting in different hydraulic resistance and consequently different attenuation performance (Husrin & Oumeraci 2009).

Most of the parameterised tree models used stiff structure assumption. Recent flume tests considering both stiff and flexible parameterised tree models of wetland vegetation (*Spartina alterniflora*) were carried out by Augustin et al. (2008). The stiff models were made from cylindrical wooden dowels while the flexible models were made from cylindrical polyethylene foam with deflecting angle up to 20°. Wave attenuation was investigated under breaking and non-breaking conditions for different water levels (emergent and submerged conditions). Wave transmission coefficient  $K_T$  was found to be

significantly larger by 15-20% under emergent conditions than submerged conditions. Surprisingly, flexible model dissipate slightly more energy by only 1-4% higher as compared to the rigid model.

An analytical approach to investigate the attenuation performance of mangrove forests under storm waves was carried out by Massel et al. (1999). They proposed a concept of energy dissipation by mangrove forest in the frequency domain by considering linearized drag losses. Additionally, based on field data, Massel et al. (1999) also outlined that the attenuation performance of mangrove forest is influenced not only by tree dimension and density but also by the spectral characteristics of the incident waves.

Previous studies show that parameters affecting the attenuation performance of coastal forests were treated differently. Moreover, damping performance of mangrove forests for practical applications is still largely unknown. Laboratory experiments were widely used for the derivation of hydraulic resistance (Manning roughness, drag and inertia coefficients) based on different parameterized models. For future laboratory testing, the wave attenuation by forests in terms of energy dissipations should be determined by using a physically-based parameterization of tree models.

The objective of the current study is to describe the hydraulic performance of a new parameterised mangrove model in terms of wave reflection, transmission, and dissipation coefficients ( $K_R$ ,  $K_T$ , and  $K_D$  respectively) for both breaking and non-breaking conditions. To achieve this objective, systematic laboratory experiments in the Twin Wave Flumes (TWF) of Leichtweiß-Institute, Technical University Braunschweig, Germany were carried out simultaneously in both flumes and the same wave conditions with and without forest model.

## MANGROVE PARAMETERISATION

Storm waves are generally in the order of 1-3 m and rarely reach more than 6 meters height at the shorelines (FEMA, 2005); i.e. the surge elevation is below the canopy of mature mangrove trees

(*Rhizophora sp.*). The roots and the trunk of mangroves based on field findings from recent tsunami events can be considered as stiff structures (Husrin and Oumeraci, 2009). Therefore, in this study only the bottom parts of mangroves (roots and the trunk) are parameterized based on the concept of submerged volume ratio  $V_m/V$  ( $V_m$ : volume of submerged roots,  $V$ : a control volume) (Mazda et al., 1997b).

The objective of tree parameterisation is to have a parameterised tree model which induces similar hydraulic losses as compared to the real tree. Therefore, a model with a real tree structure is needed. Three “real structure” models (called hereafter “real model” as the reference model) made of hardened clay were constructed with three different root densities. For each “real” model, three parameterised models with similar submerged volume ratio  $V_m/V$  and different cylinder size and arrangement were also constructed. All models were tested in a steady-flow flume for different water levels and flow velocities. A force transducer was mounted under the tested tree model, so that the total flow-induced force acting on the tree model can be measured directly.

One of the three parameterised models, consisting of a group of cylinders in staggered arrangement with vertically varying submerged volume ratio  $V_m/V$  similar to the ‘real’ tree model has been selected as the most appropriate parameterised model for further studies (Fig. 1). From the measurement results, the hydraulic properties are similar to the real model. For example, the relationship pattern of drag coefficient  $C_D$  and the Reynolds number,  $R_e$  was comparable to the previously reported field data by Mazda et al., (1997b). We found that the lower envelope of the drag coefficient  $C_D$  is 1.0 and the upper envelope may increase above 10 (Fig. 1). Details on the parameterisation experiments for the bottom part of mangrove can be found in Husrin and Oumeraci (2009).

## WAVE FLUME EXPERIMENTS

Laboratory experiments were performed in the TWF (2-m and 1-m wide, 90 m long, and 1.20 m deep) using the parameterised mangrove model

with the stiff structure assumption. By considering the dimension of the TWF and the generated waves, the model scale 1:25 was selected (Different from the parameterisation experiments with a scale 1:20). The parameterised tree models of a mangrove forest (*Rhizophora sp.*) were installed in a staggered arrangement on a horizontal platform with a foreshore slope ~1:20 in the 2 m wide flume. The distance between tree models (between trunk) is 15 cm or 3.75 m in prototype (tree density,  $N_s=0.06$  tree/m<sup>2</sup>). The same platform (shore model) without forest model was also constructed in the 1-m wide flume. Simultaneous measurements under the same incident wave conditions in both flumes are intended to better assess the incident wave conditions and the wave attenuation performance of the forest in the 2-m wide flume as compared to the conditions in the 1-m wide flume without the forest. In this way, the relative contribution of the forest and shore topography will be quantified for different wave conditions and forest widths.

The experiments in TWF are intended to study both global and local processes. The main objective of the global process investigations is to obtain the functional relationships between the hydraulic performance (wave reflection, wave transmission and energy dissipation) and the main forest parameters (e.g. width, density, etc.). Meanwhile, the main objective of the local process investigations is to determine the hydraulic losses induced by single trees and the entire forest based on the measurement of the flow together with the measurement of the flow-induced forces on a single tree and the entire forest. For this purpose, force transducers for the entire forest model (FT) and for a single tree in different group configurations (FTS) were installed. In this paper, only analyses results from the global process experiments are discussed.

The water depth was varied in such way that the effect of the submerged volume ratio  $V_m/V$  on the wave attenuation can be also obtained. The generated waves include a range of storm wave conditions represented by regular and irregular wave trains. Since the attenuation performance is very sensitive to the wave periods, the full range of possible wave period, including a variation of the wave height, have been investigated. All wave

conditions including wave decay and propagation through the forest were measured by wave gauges installed in front, along and behind the forest model. Current meters (ADV) and pressure transducers (PT) were also deployed along the forest model to capture the detailed processes associated with fluid-tree interaction. Table 1 shows the testing programme and Fig. 2 shows exemplarily an experimental set-up in the TWF.

### METHODOLOGY FOR THE ANALYSIS OF HYDRAULIC PERFORMANCE

Wave reflection occurs when there is an abrupt change in depths or channel widths. The analysis of the reflection coefficient ( $K_R$ ), transmission coefficient ( $K_T$ ), dissipation coefficient ( $K_D$ ) and the effects of different variables (dimensional and non-dimensional) is required to develop an efficient model for the hydraulic performance. Those coefficients are derived from the energy conservation relationship:

$$E_D = E_I - E_T - E_R \quad (1)$$

with:

$$E = \frac{1}{8} \rho g H^2 \quad (2)$$

where:

$E_I$  : Incident wave energy ( $J/m^2$ );  $E_R$  : Reflected wave energy ( $J/m^2$ );  $E_T$  : Transmitted wave energy ( $J/m^2$ );  $E_D$  : Dissipated wave energy ( $J/m^2$ );  $\rho$  : Water density ( $kg/m^3$ );  $g$  : Gravity acceleration ( $m/s^2$ );  $H$  : Wave height; mean wave height  $H_m$  for regular waves or spectral wave height  $H_{m0}$  for irregular waves (m);  $E$  : Wave energy associated with  $H$  and corresponding to  $E_I$ ,  $E_R$ ,  $E_T$  or  $E_D$  ( $J/m^2$ )

The incident ( $E_I$ ), the reflected ( $E_R$ ) and the transmitted ( $E_T$ ) wave energy components are determined from the analysis of the associated wave heights by using Eq. (2). The dissipated wave energy  $E_D$  is then calculated according to Eq. (1). By defining the reflection, transmission and dissipation coefficient as:

$$K_T = \sqrt{\frac{E_T}{E_I}}, K_R = \sqrt{\frac{E_R}{E_I}}, K_D = \sqrt{\frac{E_D}{E_I}} \quad (3)$$

The energy conservation relationship (Eq. (1)) can be rewritten in terms of energy coefficients as:

$$K_R^2 + K_T^2 + K_D^2 = 1 \quad (4)$$

The unknown dissipation coefficient  $K_D$  follows from Eqs. (1) until (4) as:

$$K_D = \sqrt{1 - (K_T^2 + K_R^2)} \quad (5)$$

where:

- $K_D$  : Dissipated wave coefficient (-)
- $K_R$  : Reflected wave coefficient (-)
- $K_T$  : Transmitted wave coefficient (-)

The measured waves (regular and irregular waves) in the flume are the result of the superposition of both incident and reflected waves due to the presence of shore platform and the forest model. In order to distinguish between the incident and the reflected waves, the methodology to separate incident waves and reflected waves using a least square method proposed by Mansard and Funke (1980) was implemented.

### RESULTS AND ANALYSES

The determination of reflection, transmission and dissipation coefficients ( $K_R$ ,  $K_T$ ,  $K_D$ ), the effects of relative water depth  $h/L$  and relative forest width  $B/L$ , discrimination between energy dissipation due to forest and shore topography, and the effect of different breaking locations on wave energy transmission are required for a proper interpretation and assessment of the wave attenuation performance of the forest model. The characteristics of the incident waves are first identified, classified and systematically analysed with respect to the processes associated with wave transformation, wave nonlinearity, incipient wave breaking and breaking locations, including the effect of the forest on these processes.

#### Wave Evolution and Characteristics

The characteristics of wave propagation along the shore platform and through the forest model are

the main concern in the analyses. Therefore, the following four regions are considered throughout the analyses (Fig. 3):

- Region 1 (foreshore slope): the regions where most of incident waves break. Therefore, this region is divided into 5 different sections: 1a, 1b, 1c, 1d, and 1e.
- Region 2 (flat shore): a flat region in front of the forest model.
- Region 3 (within forest): this region varies for different forest widths (four widths tested).
- Region 4 (behind the forest): region of wave attenuation due to the presence of the forest models.

The characteristics of the generated regular waves (mean wave height  $H_m$  and wave length  $L$ ) in the wave flume depend on given wave periods  $T$  and water depths  $h$ . The tested water depths are  $h=0.415-0.615$  m (see Fig. 2c). The generated wave heights during the experiments were  $H = 0.04 - 0.2$  m and wave period  $T = 0.7 - 2.5$  s in the model or  $H = 1 - 5$  m and  $T = 3.5 - 12.5$  s in prototype (based on Froude similitude). According to the signals recorded by the individual wave gauge and wave gauge arrays 1 and 2 (see Figs. 2a and 2b), the regular waves were sinusoidal. When the waves reach the shore platform, they were amplified by shoaling processes and the shape of the waves slightly changes. The trough becomes flatter and the crest steeper. Some of the waves broke along the slopes (Region 1) and while others broke along the flat shore in front of the forest model (Region 2). In few cases, non-breaking waves were observed mainly for the conditions when the wave periods are smaller and where the water level was the highest at  $h=0.615$  m (see Fig. 2c).

Inside the forest, regular patterns of the measured waves were still observed. However, higher frequency signals were also observed due to wave-forest interaction and turbulent flow. Similarly, the measured waves behind the forest consisted of waves with the same frequency as the incident waves and higher frequency components.

The irregular waves in the wave flume were generated based on JONSWAP wave spectrum with variation of significant wave height  $H_{m0}$  and peak wave period  $T_p$  were similar as for the regular waves. Breaking wave locations varied over a wider range than for regular wave cases. For irregular waves, the waves started to break from the shore slope until behind the forest model (From Region 1 until Region 4). For each single test, the breaking locations were more or less covering these four regions with different occurrence frequency for each region depending on the given water depth  $h$ . However, breaking waves mostly occurred along the slope.

Similar to the case of regular waves, the propagated waves through the forest model resulted in highly turbulent flows and wave components with higher frequencies (higher harmonics). These processes were observed throughout the experiments as clearly shown from the measured signal in frequency domain. The wave energy decreases as the frequency bands are wider for the measured waves inside the forest and behind the forest model (regions 3 and 4). Characteristics of recorded wave signals before the foreshore slope and along the entire shore platform are shown in Fig. 3 for both regular and irregular waves.

### **Preliminary Analysis of Hydraulic Performance**

The analysis was first carried out to look at the statistical characteristics of analyzed wave data in terms of  $K_R$ ,  $K_T$ , and  $K_D$  as a function of water depths, breaking/non-breaking conditions, and forest/shore topography models. The quantitative analysis is sorted based on maximum and minimum values of  $K_R$ ,  $K_T$ , and  $K_D$  for four different water depths. For each water depth, 22 tests are performed with different wave periods and wave heights.

The reflection coefficients,  $K_R$  are generally almost constant for all cases (different forest widths, water depths, breaking and non-breaking conditions, regular and irregular waves) for both shore models with forest (FM&SM) and without forest (SM). Non-breaking conditions give slightly smaller reflection as compared to the

breaking conditions. For example; for the case of reflection due to forest model and shore model (FM&SM) the reflection coefficients of breaking conditions are 13% higher as compared to non-breaking conditions (Fig. 4a). This occurs due to non-breaking waves belong to mostly deeper water depths allowing wave energy to be transmitted over the shore platform. For shallower water depths, the foreslope reflects a relatively larger portion of the incident waves. Nearly-constant values of  $K_R$  in all cases are due to the fact that the frontal areas of different forest width (B) from the forest model are always similar.

Forest widths (B) and water depths (h) largely affect transmission coefficient  $K_T$ .  $K_T$  values vary greatly from the shallowest water depth,  $h=0.465$  m to the deepest  $h=0.615$  m. The transmission coefficients for non-breaking conditions are always higher than breaking conditions. For example, for the case of irregular waves (shore model with forest, non-breaking condition,  $h=0.465$ m), the transmission coefficients are  $K_T=0.30$  for  $B=0.75$ m and  $K_T=0.07$  for  $B=3.0$ m ( $K_T$  reduces by 76%) (Husrin et al., 2009). Similarly, the increase of water depth can increase the transmission coefficient by 88% (Irregular waves, Non-breaking,  $B=3.0$ m) (Fig. 4b).

The role of shore topography and the forest can be clearly observed from the dissipation coefficients ( $K_D$ ).  $K_D$  as a function of  $K_T$  and  $K_R$  (see Eq. 5) shows higher values for smaller water depth due to the fact that in these conditions  $K_R$  and  $K_T$  are small. As reflection coefficients remain nearly constant for different water depth, the transmission coefficients and breaking conditions become the main factors affecting the dissipation coefficients,  $K_D$ .  $K_D$  values decrease as  $K_T$  values increase. It is also clear that shore topography dissipates more wave energy as compared to the results with forest model (Fig. 5).

The analyses based on maximum and minimum values are still too rough and a further detailed analysis is needed by using non-dimensional parameters to provide a more effective correlation for dependent dimensional variables such as forest width B, water depth h, and wave length L. Based on these single parameters, the following dimensionless parameters are considered to be

most relevant for further analysis of  $K_R$ ,  $K_T$ , and  $K_D$ :

$$K_R, K_T, K_D = f\left(\frac{B}{L}, \frac{h}{L}\right) \quad (6)$$

Where;  $B/L$  : Relative forest width (-);  $h/L$  : Relative water depth (-)

### Reflection Performance

The analysis of wave reflection is performed for four forest widths (B), four water depths (h) and different wave conditions. The reflection coefficient  $K_R$  is plotted versus  $B/L$  for different water depths. The figures show that for a given value of forest width, the measured reflection coefficient slightly increases with decreasing water depth. This is in agreement with the results found by Muttray et al. (2006) for the cases of rubble mound breakwaters. However, the effect of forest width B on wave reflection is almost negligible for relative forest widths  $B/L > 1.0$  as shown exemplarily in Fig. 6 for Irregular wave tests. This is due to the fact that the forest models have a similar frontal area which seems to govern the reflection performance and that the effect of wave-wave interaction inside the forest is negligibly small for larger  $B/L$  values which is also in line with experimental results using wave absorbers (Oumeraci and Koether, 2009). Breaking locations, however, do influence the reflection coefficient. Similar results are also observed for regular wave tests.

Though it can be seen from Fig. 6a that the waves are slightly reflected from the foreshore slope, but from Fig. 6b, the effect of forest on wave reflection is found to be almost negligible. It should be noted that in these cases, the forest that consists of only the bottom part of the tree does not contribute noticeably to wave reflection. So far, studies on wave reflection only due to forest are not available in the literature. The available references (e.g. Harada et al., 2000) do not explicitly mention reflections due to the forest.

Wave reflection is also affected by the location of breaking wave along the shore platform. This is clearly observed in the cases of regular waves where the breaking locations can be clearly

identified (Fig. 7). The reflection coefficient ( $K_R$ ) increases with the increasing distances between forest and breaking location. For non-breaking wave conditions, reflection coefficient  $K_R$  generally tends to be smaller compared to breaking wave conditions. This is rather surprising result is due to the fact that most wave energy for non-breaking conditions is transmitted.

### Transmission Performance

The transmission coefficient is defined as the ratio of the transmitted wave height to the incident wave height (see Eq. 3). The shallow water depth at and behind the forest caused a change in the shape of wave energy spectra compared to those in deep water and in front of the forest (Fig. 3).

The transmission coefficients ( $K_T$ ) are compared for both shore model with forest (FM&SM) and shore model without forest (SM). From statistical analyses, it can also be seen that the transmission coefficients increases with water depth for both regular and irregular waves. Breaking wave locations also influence wave transmission. Fig. 8 shows that  $K_T$  is higher for non-breaking cases while for breaking waves,  $K_T$  decreases as incipient breaking is located farther from the forest. It means also that the steeper waves are transmitted less due to most of their energy has been dissipated by the foreshore slope.

$K_T$  is plotted as a function of non-dimensional parameters  $B/L$  and  $h/L$  in Fig. 9 and Fig. 10 respectively. The waves are effectively reduced, and the transmission coefficients of the two arrangements (with forest and without forest) exhibit a significant difference (Fig. 9). Fig. 10 illustrates the influence of the forest width on transmission coefficient  $K_T$  as a function of  $h/L$ . In this figure the influence of forest width on wave transmission is clearly observed. In general, a larger water depth allows more transmission comparatively to a lower water depth. The width of the forest reduces the transmitted wave significantly up to 35%.

### Dissipation Performance

Dissipation coefficient  $K_D$  is plotted in Fig. 11 as a function of relative water depth  $h/L$  for all non-

breaking and breaking wave conditions. In all cases dissipation coefficient  $K_D$  decays with increasing relative water depth  $h/L$ . Since forest width has a direct influence on the transmission coefficient and insignificant effect on the reflection coefficient, so the dissipation coefficient is directly related to the transmission coefficient.

It is also important to notice that the dissipation coefficient reaches its maximum for smaller relative depths and  $h/L$  for all tested forest widths. However, as  $h/L$  increases, the effect of forest width  $B$  on wave energy dissipation becomes increasingly large.

The results shown in Fig. 12 describe the total energy dissipated due to both shore topography (shore model, SM), mangrove forest (forest model, FM) and combination of both (FM&SM). In order to discriminate between the part dissipated by shore topography and that dissipated by the forest, it is also necessary to analyse the result of the simultaneously performed tests in the 1-m wave flume (only shore model). While this analysis provides the contribution of the shore topography only to the total energy losses, the analysis of the tests in the 2-m flume provides both contributions together (forest and shore topography). Therefore, the dissipation only due to forest can be expressed as follow:

$$K_D(\text{forest}) = K_D(\text{forest + shore}) - K_D(\text{shore}) \quad (7)$$

Exemplarily results for the tests with water depth  $h = 0.615$  m and forest width  $B = 0.75$  m and  $B=3.0$  m are given in Fig. 12 for different relative forest widths  $B/L$  under both breaking and non-breaking wave conditions, showing that the contribution of the forest is not significant for smaller  $B/L$ -values, but considerably increases with increasing  $B/L$ . By increasing for instance the forest width  $B/L$  from 0.5 to 4.0, the dissipation coefficient by the forest increases from about 0.08 to about 0.2 (70%) while that due to shore topography only decreases from about 0.9 to 0.65 (28%) (Fig. 12b). This explains the apparent paradox observed in the results of the tests in the 2-m wave flume which provide a total energy dissipation (shore and forest) slightly decreasing

with increasing B/L. A similar behaviour was also observed for other water depth conditions and forest widths B as well as for regular waves.

### DISCUSSION OF KEY RESULTS

From the analyses above, general attenuation performance of forest model and shore model in terms of  $K_R$ ,  $K_T$ , and  $K_D$  has led to the following key results:

- **Wave reflection** is primarily caused by the shore topography and depends significantly on the wave breaking conditions and breaking locations. The contribution of the forest itself to wave reflection is almost negligible, though it slightly increases with increasing relative water depth h/L. This result is in line with the experiments carried out by Harada et al. (2000) using artificial porous media where the reflection coefficient increases by about 20% for the case of tsunami-like wave.
- **Wave transmission** is determined by both shore topography and forest, showing the necessity to discriminate between both effect in order to assess correctly the transmission coefficient of the forest itself. As expected, transmission coefficient  $K_T$  generally decreases with decreasing relative water depth h/L and increasing relative forest width B/L. The wave transmission behaviour involving both breaking and non-breaking conditions are similar to the previously reported experimental data using cylindrical dowels by Augustin et al. (2008).
- **Wave energy dissipation**, like wave transmission, is caused by both shore topography and forest. The energy dissipation patterns by mangrove model are in agreement with the field measurements of Mazda et al. (1997a) and Mazda et al. (2006), where the effect of forest density is comparable to the effect of forest width in reducing the incident waves. Moreover, the effect of shore topography in our results is clearly distinguished and physically more meaningful

by the inclusion of non-dimensional parameters as a function of forest width, water depth and wave period. As wave reflection due to the forest is negligibly small, wave energy dissipation and wave transmission are strongly related, so that dissipation coefficient  $K_D$  can be directly calculated from transmission coefficient  $K_T$  through the approximate relationship:

$$K_D = \sqrt{1 - K_T^2} \quad ; \text{ valid for } K_R \sim 0 \quad (8)$$

Many of the results which have been achieved yet were expected from the qualitative point of view, but less from the quantitative view point. The most striking results, however, consist in the relative contributions of the forest and shore topography to wave reflection coefficient  $K_R$ , transmission coefficient  $K_T$  and dissipation coefficient  $K_D$  and on how these contributions are affected by relative water depth h/L and relative forest width B/L.

### CONCLUSIONS

The hydraulic performance of mangrove forest (in this case the bottom part of the tree: roots and trunk) of different forest widths B is systematically tested under both regular and irregular wave trains for different water depths h and breaking locations. The analysis is performed in terms of wave reflection, wave transmission and energy dissipation. The results have allowed to identify the two most relevant non-dimensional parameters which affect reflection coefficient  $K_R$ , dissipation coefficient  $K_D$  and transmission coefficient  $K_T$  for a given forest density; namely relative water depth h/L (h: water depth, L: wave length of incident wave) and relative forest width B/L (B: forest width). Overall, the wave damping performance due to both forest and shore topography increases with decreasing water depth h/L and increasing forest width B/L. For smaller water depth h/L the contribution of the forest to wave damping is negligibly small, but becomes increasingly large with increasing water depth h/L and increasing forest width B/L. The results have revealed that the combined effect of relative water depth h/L and relative forest width B/L on the relative contribution of forest and shore

topography on wave reflection ( $K_R$ ), transmission ( $K_T$ ) and dissipation ( $K_D$ ) is even more complex and needs a more detailed analysis. Nevertheless, the results achieved so far clearly reveals novel and equally vital aspects in the sense that the modeling and arrangement of the wave attenuation performance of coastal forests have to be put on new grounds by taking into account properly the relative effect of the cross-shore topography, the wave evolution modes on the foreshore and inside the forest, including the combined effect of both relative water depth  $h/L$  and relative forest width  $B/L$ .

Improvement is still required to have complete understanding of the attenuation performance of storm waves by mangrove forest, such as: inclusion of mangroves canopy, trunk flexibility, variation on forest densities, different shore slopes, and other mangrove species. Furthermore, in the next stage, the investigation of local processes in which flow-induced forces were measured for individual tree models within the forest model will provide a deeper insight into the processes responsible for the flow resistance of single trees within the forest.

#### ACKNOWLEDGEMENTS

The first and the third authors are supported by the DFG within the Graduate College of TU Braunschweig (GRK 802) in “Risk Management of Natural & Civilization Hazards on Buildings & Infrastructure”, and the Alexander von Humboldt Foundation (AvH), respectively. The model experiments are supported by the *Tsunami Attenuation Performance by Coastal Forests* (TAPFOR) Project (DFG Ou 1/10-1).

#### REFERENCES

- Augustin, LN, Irish, JL, Balsmeier, G, Kaihatu, J (2008). “Laboratory measurements of wave attenuation and wave setup by vegetation”, *Proceeding of 2008 ICCE Hamburg-Germany*: pp. 324-330.
- FEMA (2005). "Mississippi Hurricane Katrina Surge Inundation and Advisory Base Flood Elevation Map Panel Overview". Federal Emergency Management Agency (<http://www.fema.gov/pdf/hazard/flood/reco> verydata/katrina/ms\_overview.pdf. Retrieved 2010-01-11.
- Harada, K, Latief, H, Imamura, F (2000). “Study on the mangrove control forest to reduce tsunami impact”, *Proceedings of 12<sup>th</sup> Congress of the IAHR-APD*, Bangkok.
- Husrin, S, & Oumeraci, H (2009). “Parameterization of coastal forest vegetation and hydraulic resistance coefficients for tsunami modelling”. *Proc. of the 4<sup>th</sup> Ann. Inter. Worksh. & Expo on Sumatra Tsunami Disast. & Recov.*, Banda Aceh, Indonesia, pp. 78-86
- Husrin, S, Hoque, A, Oumeraci, H (2009). “Hydrodynamic performance of mangrove forest under regular and irregular waves” *Internal Report*, LWI, TU Braunschweig, Germany, pp. 76.
- Mansard, EPD, & Funke, ER (1980). “The Measurement of Incident and Reflected Spectra Using a Least Squares Method”, *Proceedings of the 17<sup>th</sup> Int. Conf. on Coastal Eng*, Sidney, Australia, pp. 154–172.
- Massel, SR, Furukawa, K, Brinkman, RM (1999). “Surface waves propagation in mangrove forests”, *Fluid Dynamics Research*, 24: pp. 219-249.
- Mazda, Y, Magi, M, Ikeda, Y, Kurokawa, T, Asano, T (2006). “Wave reduction in a mangrove forest dominated by *Sonneratia* sp.” *Wetlands Ecology and Management* 14: 365–78.
- Mazda, Y, Magi, M, Kogo, M, & Hong, P (1997a). “Mangroves as a coastal protection from waves in the Tong King delta, Vietnam”, *Mangroves and Salt Marshes 1* (1997), pp. 127–135
- Mazda, Y, Wolanski, EJ, King, BA, Sase, A, Ohtsuka, D, Magi, M (1997b). “Drag force due to vegetation in mangrove swamps”. *Mangroves and Salt Marshes*, Vol. 1, No. 3, pp. 193-199.
- Muttray, M, Oumeraci, H, Oever, E (2006). “Wave reflection and wave runup at rubble mound breakwaters”, *ICCE 2006 proceeding San Diego*, USA, pp. 4314-4324
- Oumeraci, H, and Koether, G (2009). “Hydraulic Performance of a Submerged Wave Absorber for Coastal Protection”. *Nonlinear Wave Dynamics*, edited by P. Lynett, Wolrd Sci Book, pp. 31-65.
- Petryk, S, & Bosmajian, G (1975). “Analysis of flow through vegetation”, *Journal of Hydraulics Div.*, ASCE: pp. 871–884
- Walton, TLJr, & Dean, RG (2009). “Landward limit of wind setup on beaches”, *Ocean Engineering*, Vol. 36, Issues 9-10, July 2009, pp. 763-766
- Wolanski, E., M. Jones, and J. S. Bunt. (1980). “Hydrodynamics of a tidal-creek mangrove swamp system”. *Austral. J. Mari. Freshwater Res* 31: pp. 431–450

Wave types	Model values				Prototype values				Wave steepness, H/L(-)
	Water depth in front of the slope, h (m)	Forest width, B (m)	Incident wave height, H <sub>m</sub> or H <sub>m0</sub> (m)	Wave period, T or T <sub>p</sub> (s)	Water depth in front of the slope, h (m)	Forest width, B (m)	Incident wave height, H <sub>m</sub> or H <sub>m0</sub> (m)	Wave period, T or T <sub>p</sub> (s)	
Regular & Irregular Waves	0.465 0.515 0.565 0.615	0.75 1.50 2.25 3.00	0.04	0.7	11.625 12.875 14.125 15.375	18.75 37.50 56.25 75.00	1	3.5	0.052
				0.9				4.5	0.032
				1.1				5.5	0.021
			0.08	1			2	5.0	0.051
				1.2				6.0	0.036
				1.4				7.0	0.026
			0.12	1.6			3	8.0	0.020
				1.2				6.0	0.053
				1.4				7.0	0.039
			0.16	1.6			4	8.0	0.030
				1.4				7.0	0.052
				1.8				8.0	0.040
			0.20	2.0			5	9.0	0.032
				2.2				10.0	0.026
				1.5				11.0	0.021
				1.7				7.5	0.057
				1.9				8.5	0.044
				2.1				9.5	0.035
				2.3				10.5	0.029
			2.5	11.5			0.024		
			12.5	0.020					

**TABLE 1:** Testing programme for regular and irregular waves in the TWF (model scale, 1:25)

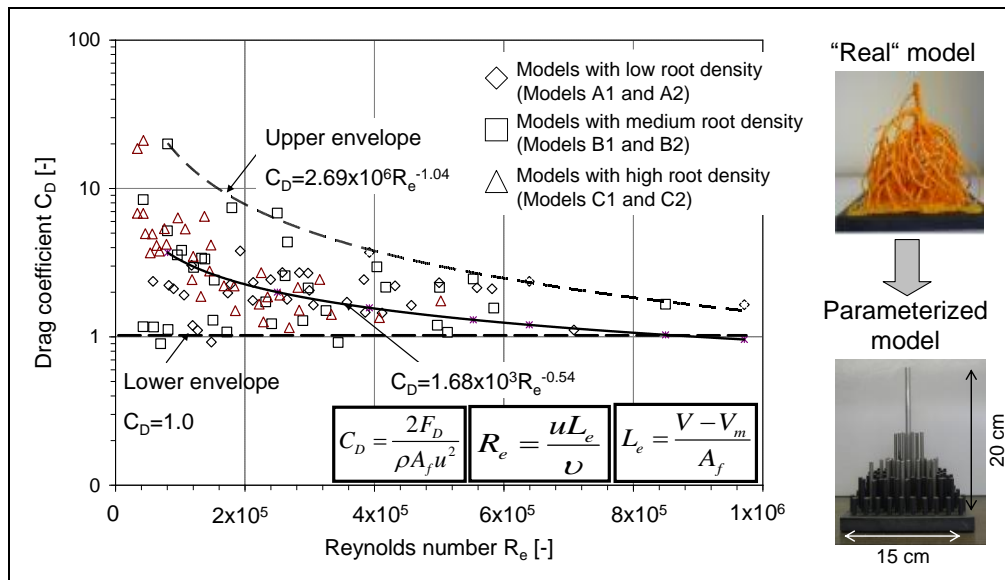


**FIGURE 1:** Laboratory results of mangrove parameterisation with stiff structure assumption

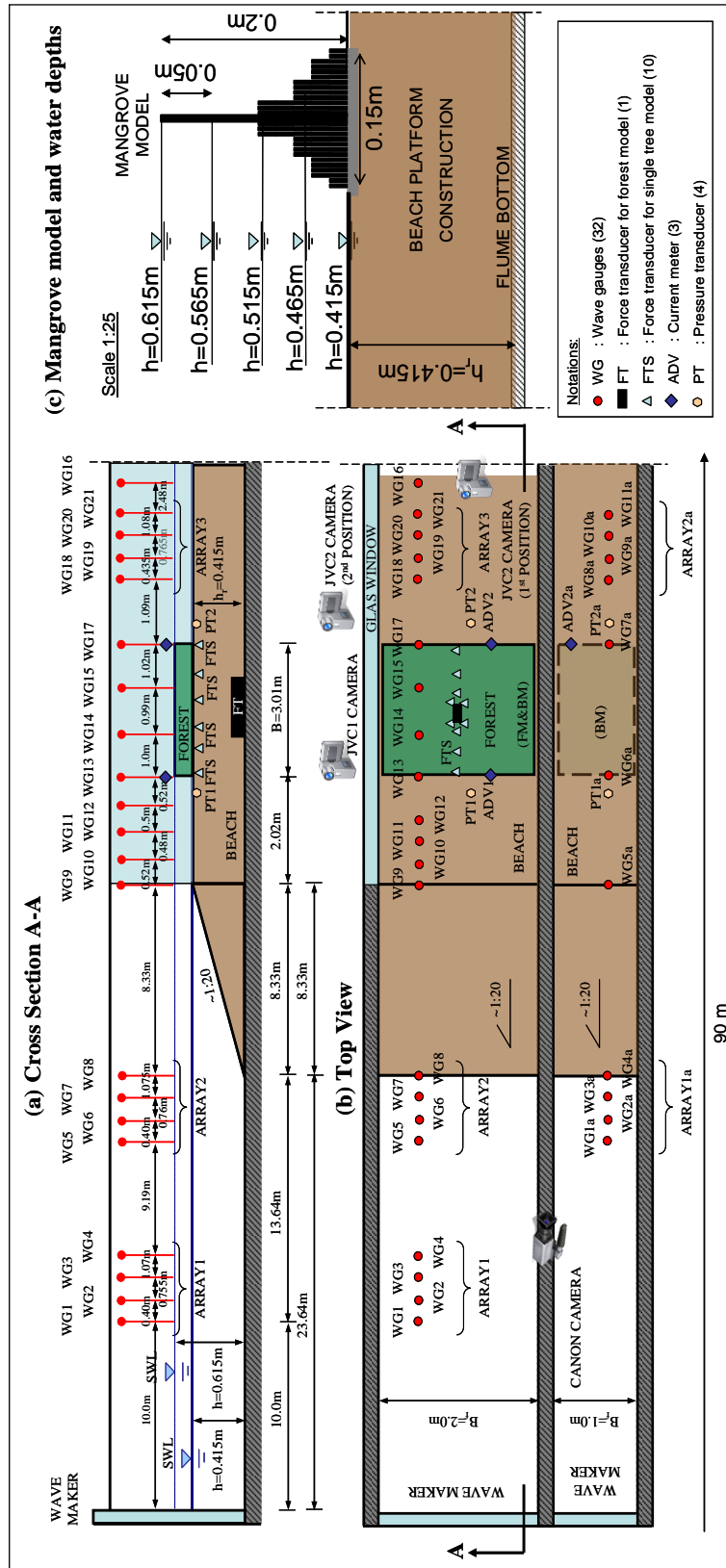
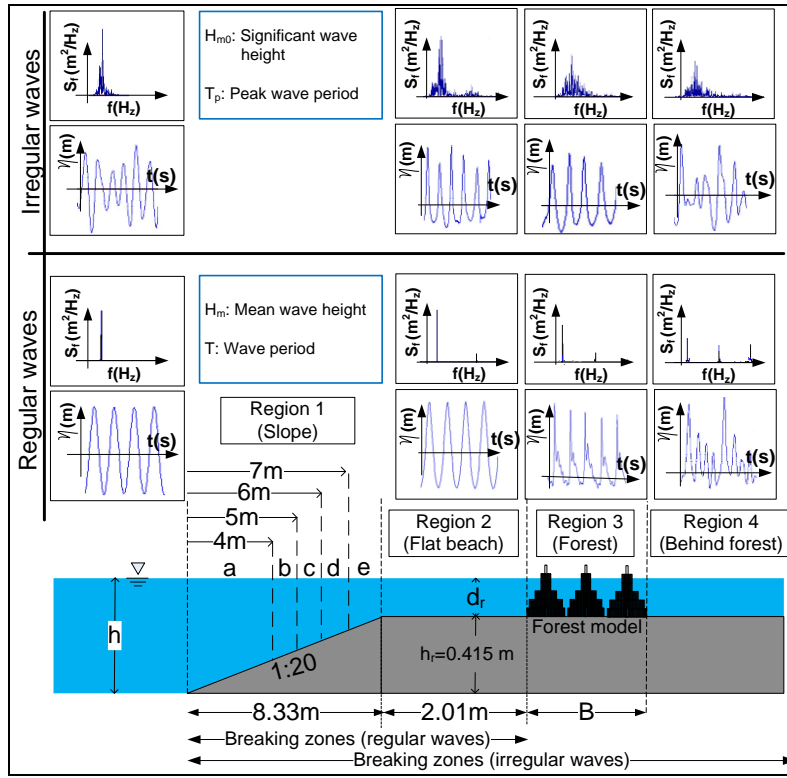
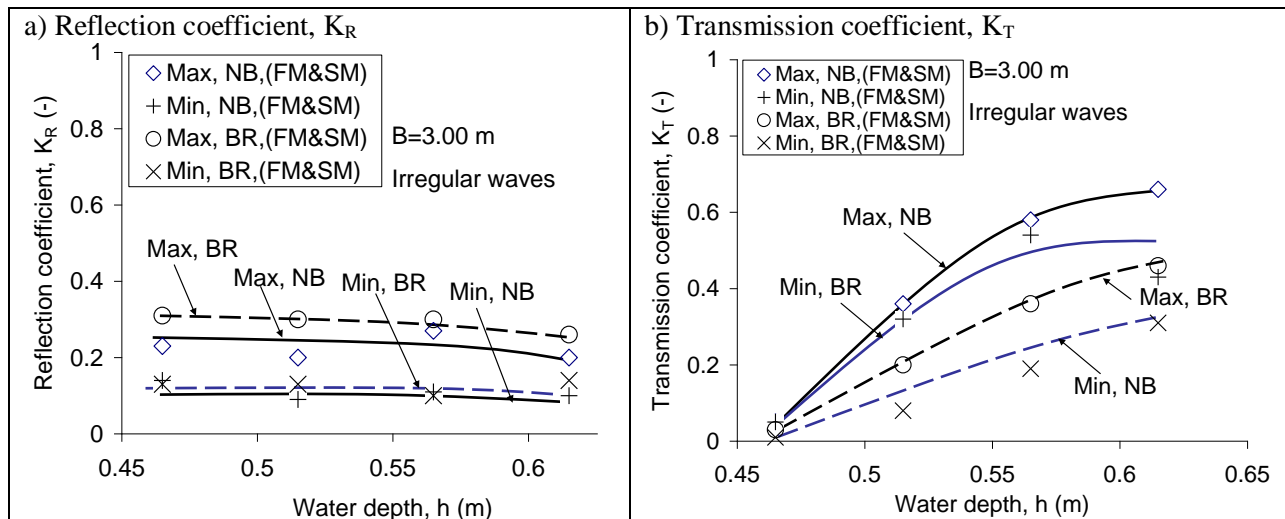


FIGURE 2: Experimental set-up in the twin wave flume (TWF)



**FIGURE 3:** Characteristics of regular and irregular waves for different regions in time and frequency domains



**FIGURE 4:** Maximum (Max) and minimum (Min) values of reflection coefficients,  $K_R$  and transmission coefficients,  $K_T$  for different water depths. NB: non-breaking; BR: breaking; FM&SM: shore model with forest model; SM: shore model

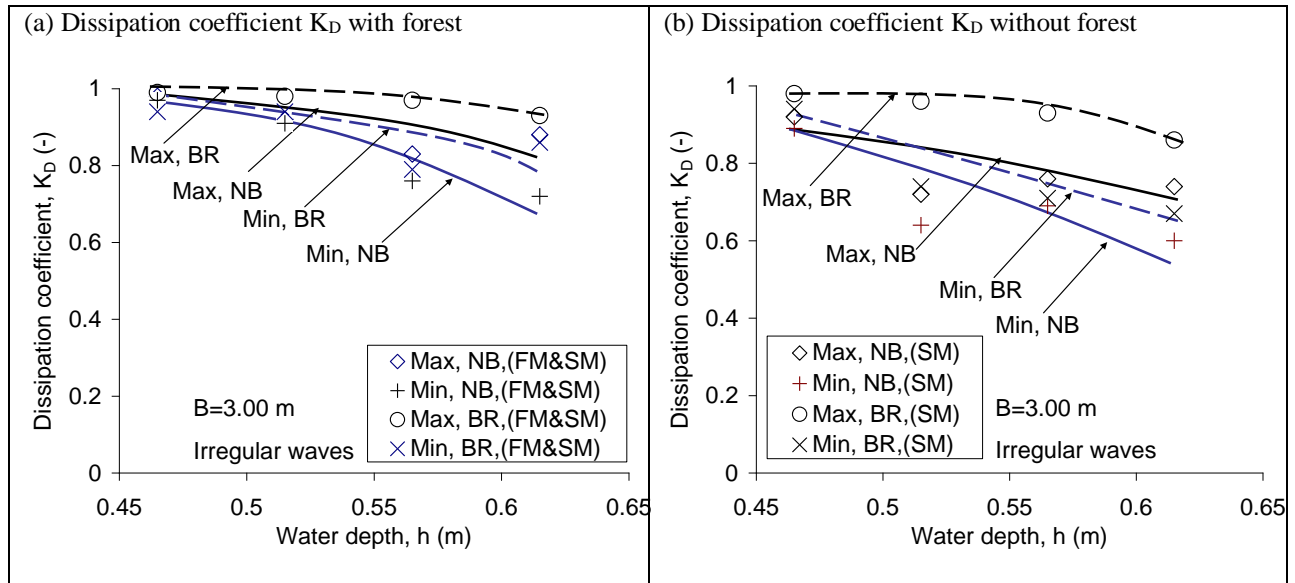


**FIGURE 5:** Maximum (Max) and minimum (Min) values of dissipation coefficients,  $K_T$  for different water depths. NB: non-breaking; BR: breaking; FM&SM: shore model with forest model; SM: shore model

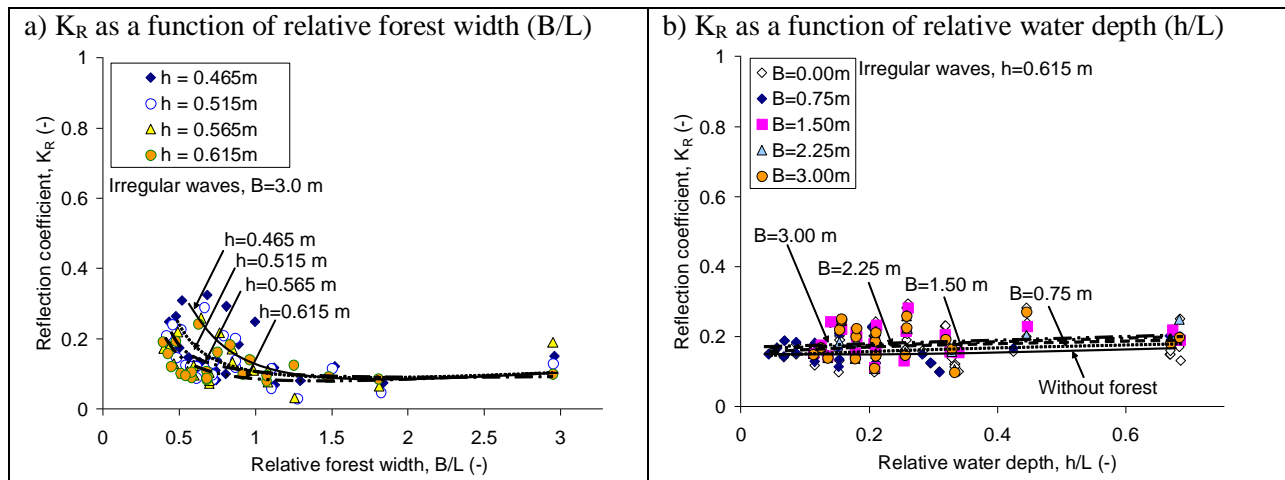


**FIGURE 6:** Effects of water depths and forest widths to the reflection coefficients ( $K_R$ )

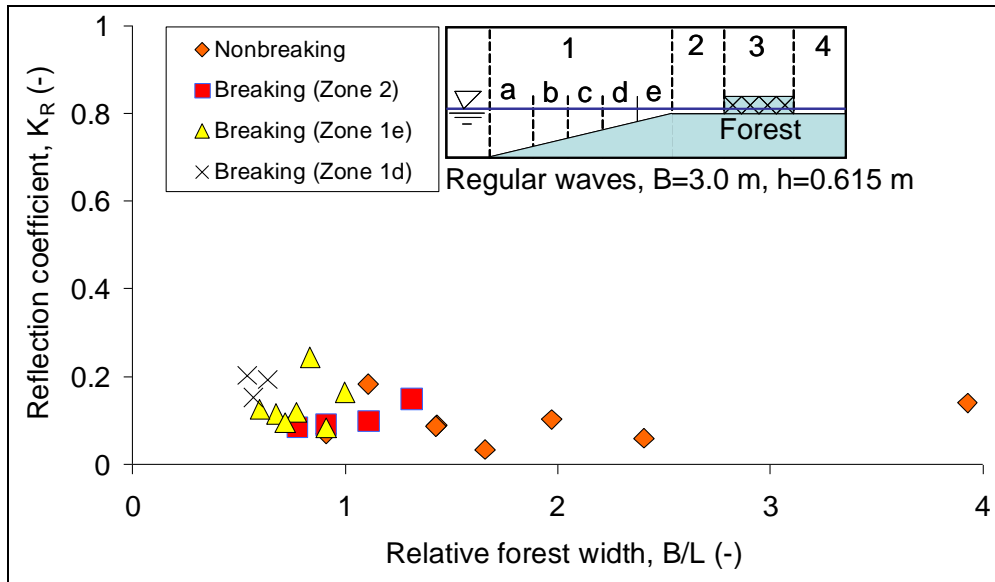


**FIGURE 7:** Reflection coefficients ( $K_R$ ) for  $B=3.0$ m and  $h=0.615$ m as a function of relative forest width ( $B/L$ ) for regular waves

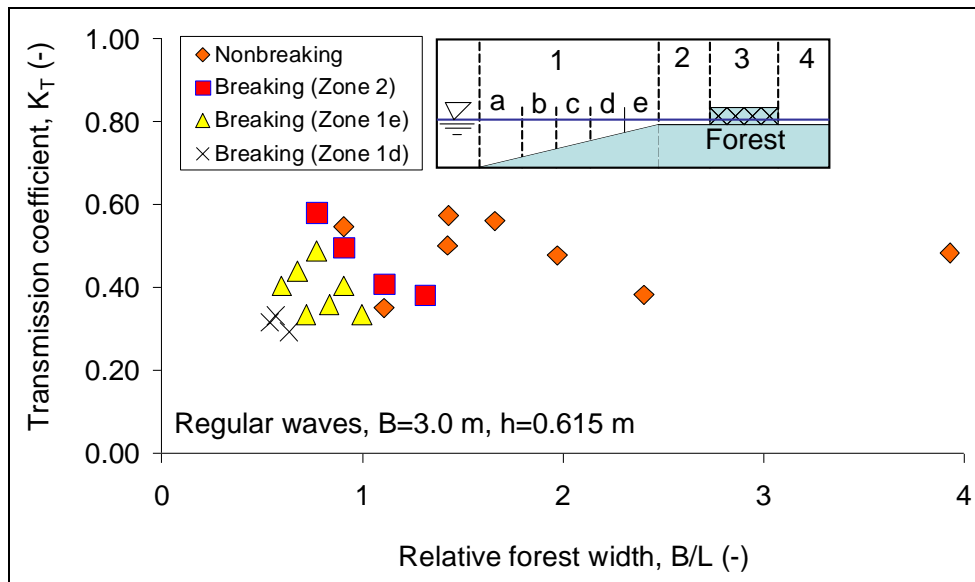


**FIGURE 8:** Transmission coefficients ( $K_T$ ) as a function of breaking wave locations and relative forest width ( $B/L$ )

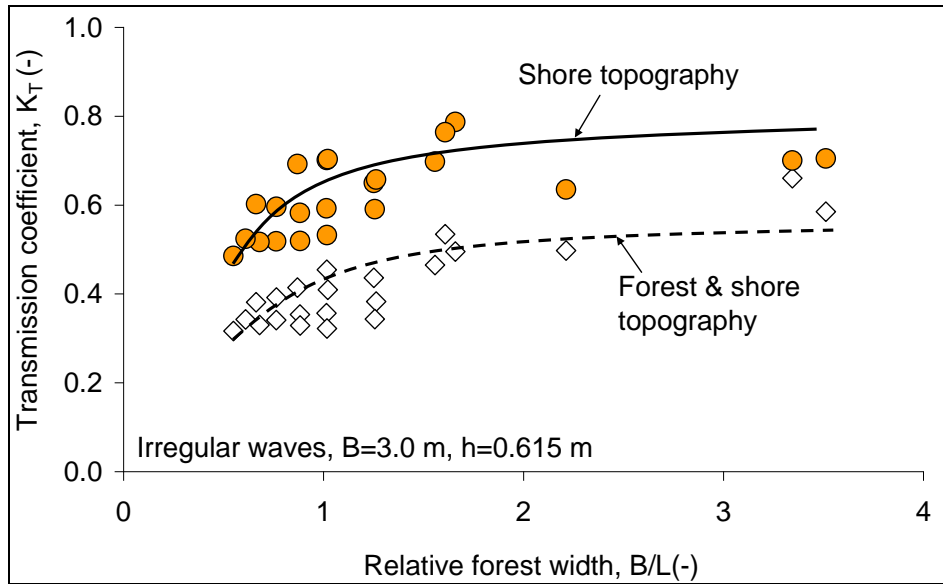


**FIGURE 9:** Transmission coefficient ( $K_T$ ) for forest and shore topography model and for only shore topography model

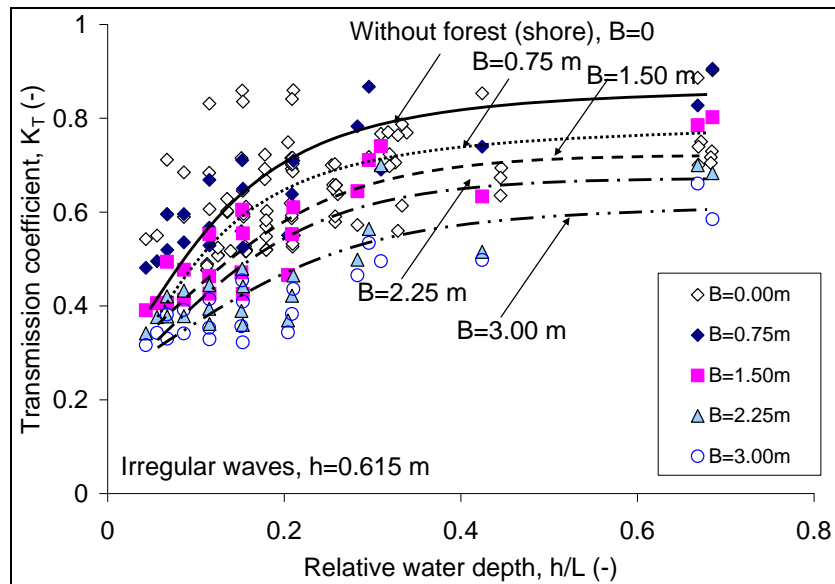


**FIGURE 10:** Transmission coefficient ( $K_T$ ) for different forest widths vs. relative water depth ( $h/L$ )

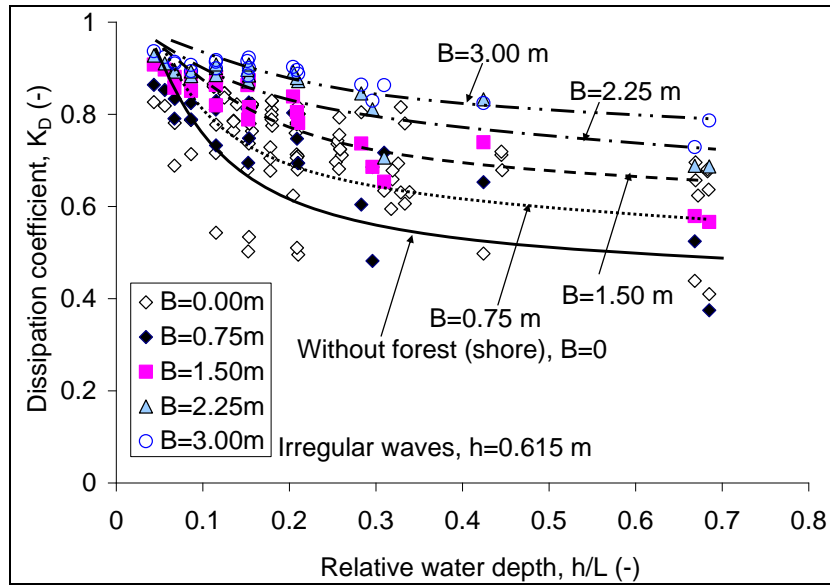


**FIGURE 11:** Dissipation coefficient ( $K_D$ ) for different forest widths vs. relative water depth ( $h/L$ )

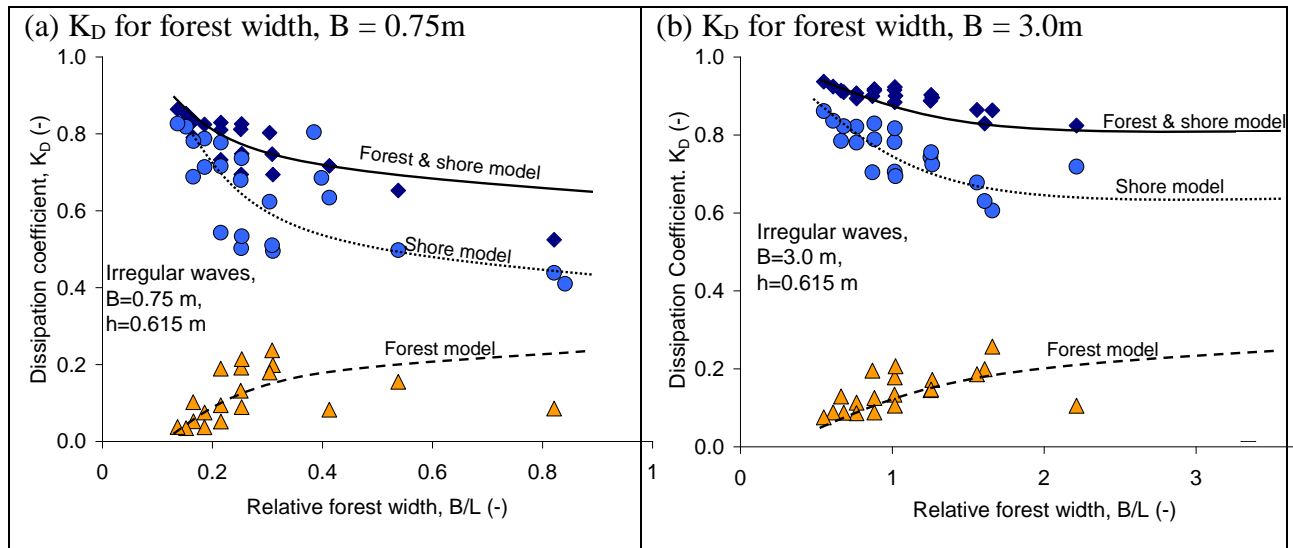


**FIGURE 12:** Variation of dissipation coefficients ( $K_D$ ) vs. relative forest width  $B/L$  for irregular waves.